

B. 研究方法

1) 遺伝子改変マウス及び軟骨細胞

前年度までに作製済みの miR-140 ノックアウトマウスと野生型を用いて各実験を行った。軟骨細胞は各遺伝子型のマウスの大腿骨及び脛骨の成長板から採取し、実験に使用した。

2) リアルタイム PCR

miR-140 ノックアウトマウスと野生型の軟骨細胞の cDNA を用いて、軟骨細胞分化の各段階のマーカー遺伝子 (*Runx2*, *Osx*, *Col10a1*, *Mmp13*)、及び miR-140 標的遺伝子候補の発現量を比較した。

3) ルシフェラーゼアッセイ

Igfbp5, *Bmp2*, *Wnt9a* の 3'-UTR に存在する miR-140 結合予測配列をルシフェラーゼ遺伝子の 3'-UTR に挿入したレポーターベクターを用いてルシフェラーゼアッセイを行った。

C. 研究結果

miR-140 ノックアウトマウスの軟骨細胞において *Igfbp5*, *Bmp2*, *Wnt9a* の 3 遺伝子の発現が亢進した。また、これらの遺伝子の 3' UTR の配列を含むレポーターベクターを作製し、ルシフェラーゼアッセイを行うと、miR-140 によってルシフェラーゼの活性が有意に減少することを見出した。以上の結果から、これらの遺伝子も miR-140 によって直接制御を受けている可能性が示唆された。

また、EMBRYS より、軟骨特異的に発現する転写関連因子を調査した結果、Fox ファミリーに属する 3 遺伝子が軟骨に特異的に発現していることが分かった。

D. 考察

Igfbp5 は *IGF1* シグナルを抑制することで増殖を抑制する因子であり、*Bmp2* は *p38* を介した軟骨細胞の増殖の促進、*Smad* を介した軟骨細胞の肥大化の両方に関与する遺伝子である。*Wnt9a* は *Bmp/Smad* 経路と同様に *Runx2* の発現を誘導することが報告されている。miR-140 ノックアウトマウスでは長管骨の伸長が阻害されているが、miR-140 はこれら遺伝子を抑制することで、軟骨細胞の増殖、肥大化の制御を行っている可能性が示唆された。

EMBRYS により軟骨分化を制御する新たな候補遺伝子として、Fox 遺伝子を同定した。これらについてはノックアウトマウスを作製し、軟骨分化における機能を明らかにしていくと共に、滑膜間葉幹細胞を用いた軟骨再生において、これら Fox 遺伝子や軟骨分化に重要な miRNA である miR-140 の挙動についても調査していく。

E. 結論

軟骨分化メカニズムの詳細な解析を行なった結果、miR-140 が *Igfbp5*, *Bmp2*, *Wnt9a* の 3 遺伝子を抑制することにより軟骨細胞の増殖、肥大化の制御を行っている可能性が示唆された。また、軟骨分化に関わる新たな遺伝子候補として Fox 遺伝子を同定し

た。

F. 健康危険情報

報告すべき健康被害、健康危険情報はない。

G. 研究発表

1. 論文発表

1. miRNAs in cartilage development.

Asahara H.

Clin Calcium. 2012; 22(5): 653-7.

2. Analysis of molecular network

in chondrocytes by WISH.

Miyaki S, **Asahara H.**

Clin Calcium. 2011; 21(6): 831-8.

H. 知的財産権の出願・登録状況

該当無し

III. 研究成果の刊行に関する一覧表

研究成果の刊行に関する一覧表

雑誌

発表者氏名	論文タイトル名	発表誌名	巻号	ページ	出版年
Horie M, DriscollMD, SampsonHW, <u>Sekiya I</u> , CaroomCT, ProckopDJ, Thomas DB.	Implantation of allogenic synovial stem cells promotes meniscal regeneration in a rabbit meniscal defect model.	J Bone Joint Surg Am	18;94(8)	701-712.	2012
NakamuraT, <u>SekiyaI</u> , <u>MunetaT</u> , HatsushikaD, Horie M, Tsuji K, Kawarasaki T, Watanabe A, Hishikawa S, Fujimoto Y, Tanaka H, Kobayashi E.	Arthroscopic, histological and MRI analyses of cartilage repair after a minimally invasive method of transplantation of allogeneic synovial mesenchymal stromal cells into cartilage defects in pigs	Cytherapy	14(3)	327-38.	2012
<u>Sekiya I</u> , Ojima M, Suzuki S, Yamaga M, Horie M, Koga H, Tsuji K, Miyaguchi K, Ogishima S, Tanaka H, <u>Muneta T</u>	Human mesenchymal stem cells in synovial fluid increase in the knee with degenerated cartilage and osteoarthritis.	J Orthop Res.	30(6)	943-9.	2012
<u>関矢一郎</u> <u>宗田 大</u>	滑膜間葉幹細胞の役割と 低侵襲な軟骨再生への応 用	雑誌 整形外科 整形トピックス	Vol.63, No.3,	228	2012
<u>関矢一郎</u> <u>宗田 大</u>	変形性膝関節症をめぐる 進歩 滑膜由来の幹細胞による 再生医療	Bone Joint Nerve	Vol.2, No.1,	159-165	2012

関矢一郎 宗田 大	再生医学のいま 基礎 研究から臨床への展開 に向けて 滑膜幹細胞を用いた関 節軟骨再生	治療	Vol.93, No.8	1784-1793	2011
関矢一郎	滑膜間葉幹細胞を用い た関節軟骨再生	クリニカルカル シウム	Vol.21	p83-93	2011
関矢一郎	軟骨再生の概要と応用の 可能性	日本医事新報	No. 4548	p59-61 No. 4548	2011
Jang SH, Lim JW, Morio T , Kim H.	Lycopene inhibits Helicobacter pylori-induced ATM/ATR-dependent DNA damage response in gastric epithelial AGS cells.	Free Radical Biol. Med.	52	607-615	2012
Lee SW, Kim JH, Park MC, Park YB, Chae WJ, Morio T , Lee DH, Yang SH, Lee SK, Lee SK, Lee SK,	Alleviation of rheumatoid arthritis by cell-transducible methotrexate upon transcutaneous delivery.	Biomaterials	33	1563-72	2012
Nakamura K. Du L. Tunuguntla R. Fike F. Cavalieri S. Morio T . Mizutani S. Brusco A. Gatti RA.	Functional characterization and targeted correction of ATM mutations identified in Japanese patients with ataxia-telangiectasia.	Hum Mutat.	33	198-208	2012

清水則夫	細胞治療のウイルス安全性確保に関する取り組み	医薬品の品質管理とウイルス安全性	4章	102 ~111	2011
清水則夫	病原微生物の網羅的検出法の開発と応用	医薬品の品質管理とウイルス安全性	7章	287 ~294	2011
Sugita S <u>Shimizu N</u> Watanabe K Katayama M Horie S Ogawa M Takase H Sugamoto Y Mochizuki M	Diagnosis of bacterial endophthalmitis by broad-range quantitative PCR.	Br.J.Ophthalmol.	95	345-349	2011
Ng S, Selvarajan V, Hung G, Zhou J, L Feldman A, Low M, Kwong Y, <u>Shimizu N</u> , Kagami Y, Aozasa K.	Activated oncogenic pathways and therapeutic targets in extranodal nasal-type NK/T cell lymphoma revealed by gene expression profiling	J Phatol	233	496-510.	2011
Abe T, Segawa Y, Watnabe H, Yotoriyama T, Kai S, Yasuda A, <u>Shimizu N</u> , Tojo N.	Point-of-Care Testing System Enabling 30-min Detection of Influenza Genes.	LAB CHIP	11	1166-1167	2011

Yagasaki H, Kato M, Shimizu N , Shichino H, Chin M, Mugishima H.	Autoimmune hemolytic anemia and autoimmune neutropenia in a child with erythroblastopenia of childhood (TEC) caused by human herpesvirus-6 (HHV6).	Ann Hematol	90(7)	851-852	2011
Watanabe A, Tagawa H, Yamashita J, Teshima K, Nara M, Iwamoto K, Kume M, Kameoka Y, Takahashi N, Nakagawa T, Shimizu N , Sagawa K.	The role of microRNA-150 as a tumor suppressor in malignant lymphoma. Leukemia	Leukemia	25(8)	1324-1334	2011
Sugita S, Ogawa M, Inoue S, Shimizu N , Mochizuki M.	Diagnosis of ocular toxoplasmosis by two polymerase chain reaction (PCR) examinations: qualitative multiples and quantitative real-time	Jpn J Ophthalmol.	55(5)	495-501.	2011
Sugita S, Komori K, Ogawa M, Watanabe K, Shimizu N , Mochizuki M.	Detection of Candida & Aspergillus species DNA using broad-range real-time PCR for fungal endophthalmitis.	Graefe Arch Clin Exp	250	391-398	2012
Ng S, Yan J, Huang G, Selvarajan V, Tay J, Lin B, Bi C, Tan J, Kwong Y, Shimizu N , Aozasa K, Chng W.	Dysregulated MicroRNAs Affect Pathways and Targets of Biological Relevance in Nasal-type Natural Killer / T-cell Lymphoma	Blood	118	4919-4929	2011

Imadome K, Yajima M, Arai A, Nakazawa A, Kawano F, Ichikawa S, <u>Shimizu N.</u> Yamamoto N, Morio T, Ohga S, Nakamura H, Ito M, Miura O, Komano J, Fujiwara S.	Novel Mouse Xenograft Models Reveal a Critical Role of CD4+ T Cells in the Proliferation of EBV-Infected T and NK Cells.	PLoS Pathogens	7(10)	e1002326	2011
Kuwana Y, Takei M, Yajima M, Imadome K, Inomata H, Shiozaki M, Ikumi N, Nozaki T, Shiraiwa H, Kitamura N, Takeuchi J, Sawada S, Yamamoto N, <u>Shimizu N.</u> Ito M, Fujiwara S.	Epstein-Barr Virus Induces Erosive Arthritis in Humanized Mice.	PloS ONE	6(10)	e26630	2011
Ramakrishnan R, Donahue H, Garcia D, Tan J, <u>Shimizu N.</u> Rice A, D.Ling P.	Epstein-Barr virus BART9 miRNA modulates LMP1 levels and affects growth rate of nasal NK T cell lymphomas.	PLoS ONE	6(11)	e27271	2011

Hara-Miyauchi C, Tsuji O, Hanyu A, Okada S, Yasuda A, Fukano T, Akazawa C , Nakamura M, Imamura T, Matsuzaki Y, Okano HJ, Miyawaki A, Okano	Bioluminescent system for dynamic imaging of cell and animal behavior.	Biochem Biophys Res Commun	419	188-193	2012
Miyahara K, Kato Y, Koga H, Dizon R, Lane GJ, Suzuki R, Akazawa C , Yamatata A.	Visualization of enteric neural crest cell migration in SOX10 transgenic mouse gut using time-lapse fluorescence imaging.	J Pediatr Surg.	46	2305-2308	2011
The dual origin of the peripheral olfactory system: placode and neural crest. Katoh H, Shibata S, Fukuda K, Sato M, Satoh E, Nagoshi N, Minematsu T, Matsuzaki Y, Akazawa C , Toyama Y, Nakamura M, Okano H Miyahara K, Kato Y, Koga H, Dizon R, Lane GJ, Suzuki R, Akazawa C , Yamatata A.	The dual origin of the peripheral olfactory system: placode and neural crest.	Mol Brain	Sep 23	4-34	2011
Asahara H	miRNAs in cartilage development	Clin Calcium	22(5)	653-7	2012

Miyaki S, <u>Asahara H.</u>	Analysis of molecular network in chondrocytes by WISH	Clin Calcium	21(6)	831-8	2011
<u>Nakamura N.</u> , Takeuchi R., Sawaguchi T., Ishikawa H., <u>Saito T.</u> , Goldhahn, S.	Cross-cultural adaptation and validation of the Japanese Knee Injury and Osteoarthritis Outcome Score (KOOS).	J Orthop. Sci.	16-Jul		2011
Inaba Y, Ozawa R, Imagawa T, Mori M, Hara Y, Miyamae T, Aoki C, <u>Saito T.</u> , Yokota S.	Radiographic improvement of damaged large joints in children with systemic juvenile idiopathic arthritis following tocilizumab treatment.				
Sakai T, Koyanagi M, Nakata K, Fujisaki H, Yamagata T, Hidaka K, Suzuki Y, <u>Nakamura N.</u>	Posterior shear force and posterior tibial displacement using a sling bridge in patients with posterior cruciate ligament insufficiency.	Br J Sports Med.	45(4)	370	2011
Tanaka Y, Shino K, Horibe S, <u>Nakamura N.</u> , Nakagawa S, Mae T, Otsubo H, Suzuki T, Nakata K.	Triple-bundle ACL grafts evaluated by second-look arthroscopy.	Knee Surg Sports Traumatol Arthrosc.	24-May		2011
Gobbi A, Mahajan V, Karnatzikos G, <u>Nakamura N.</u>	Single- versus Double-bundle ACL Reconstruction: Is There Any Difference in Stability and Function at 3-year Followup?	Clin Orthop Relat Res.	11-Jun		2011

Shino K, Mae T, Nakamura N.	Surgical Technique: Revision ACL Reconstruction With a Rectangular Tunnel Technique.	Clin Orthop Relat Res.	28-Jun		2011
Kita K, Horibe S, Toritsuka Y, Nakamura N. Tanaka Y, Yonetani Y, Mae T, Nakata K, Yoshikawa H, Shino K.	Effects of medial patellofemoral ligament reconstruction on patellar tracking.	Knee Surg Sports Traumatol Arthrosc	15-Jun		2011
ISAKOS Scientific Committee, Audigé L, Ayeni OR, Bhandari M, Boyle BW, Briggs KK, Chan K, ChaneyBarclay K, Do HT, Ferretti M, Fu FH, Goldhahn J, Goldhahn S, Hidaka C, Hoang-Kim A, Karlsson J, Krych AJ, LaPrade RF, Levy BA, Lubowitz JH, Lyman S, Ma Y, Marx RG, Mohtadi N, Marcheggiani Muccioli GM, Nakamura N. Nguyen J, Poehling GG, Poehling GG, Rosenberg N, Shea KP, Sohani ZN, Soudry M, Voineskos S, Zaffagnini S.	A practical guide to research: design, execution, and publication. Editors: Jón Karlsson, M.D., Ph.D., Robert G. Marx, M.D., M.Sc., F.R.C.S.C., Norimasa Nakamura, M.D., Ph.D., and Mohit Bhandari, M.D., Ph.D., F.R.C.S.C.	Arthroscopy. 2011 Apr;27(4 Suppl):S1-112.	27-Apr		2011

IV. 研究成果の刊行物・別刷

Implantation of Allogenic Synovial Stem Cells Promotes Meniscal Regeneration in a Rabbit Meniscal Defect Model

Masafumi Horie, MD, PhD, Matthew D. Driscoll, MD, H. Wayne Sampson, PhD, Ichiro Sekiya, MD, PhD, Cyrus T. Caroom, MD, Darwin J. Prockop, MD, PhD, and Darryl B. Thomas, MD

Investigation performed at Scott & White Memorial Hospital and the Texas A&M Health Science Center College of Medicine Institute for Regenerative Medicine, Temple, Texas

Background: Indications for surgical meniscal repair are limited, and failure rates remain high. Thus, new ways to augment repair and stimulate meniscal regeneration are needed. Mesenchymal stem cells are multipotent cells present in mature individuals and accessible from peripheral connective tissue sites, including synovium. The purpose of this study was to quantitatively evaluate the effect of implantation of synovial tissue-derived mesenchymal stem cells on meniscal regeneration in a rabbit model of partial meniscectomy.

Methods: Synovial mesenchymal stem cells were harvested from the knee of one New Zealand White rabbit, expanded in culture, and labeled with a fluorescent marker. A reproducible 1.5-mm cylindrical defect was created in the avascular portion of the anterior horn of the medial meniscus bilaterally in fifteen additional rabbits. Allogenic synovial mesenchymal stem cells suspended in phosphate-buffered saline solution were implanted into the right knees, and phosphate-buffered saline solution alone was placed in the left knees. Meniscal regeneration was evaluated histologically at four, twelve, and twenty-four weeks for (1) quantity and (2) quality (with use of an established three-component scoring system). A similar procedure was performed in four additional rabbits with use of green fluorescent protein-positive synovial mesenchymal stem cells for the purpose of tracking progeny following implantation.

Results: The quantity of regenerated tissue in the group that had implantation of synovial mesenchymal stem cells was greater at all end points, reaching significance at four and twelve weeks ($p < 0.05$). Tissue quality scores were also superior in knees treated with mesenchymal stem cells compared with controls at all end points, achieving significance at twelve and twenty-four weeks (3.8 versus 2.8 at four weeks [$p = 0.29$], 5.7 versus 1.7 at twelve weeks [$p = 0.008$], and 6.0 versus 3.9 at twenty-four weeks [$p = 0.021$]). Implanted cells adhered to meniscal defects and were observed in the regenerated tissue, where they differentiated into type-I and II collagen-expressing cells, at up to twenty-four weeks.

Conclusions: Synovial mesenchymal stem cells adhere to sites of meniscal injury, differentiate into cells resembling meniscal fibrochondrocytes, and enhance both quality and quantity of meniscal regeneration.

Clinical Relevance: These results may stimulate further exploration into the utility of synovial mesenchymal stem cells in the treatment of meniscal injury in large animals and humans.

The meniscus is a fibrocartilage structure functioning to increase surface contact area, absorb mechanical loads, and improve stability across the knee joint. Following injury, the human meniscus demonstrates poor healing potential

because of the largely avascular nature of its fibrocartilaginous tissue. Failure rates after attempted surgical repair remain high, ranging from 24% to 50% for isolated meniscal tears¹⁻⁸. As a result, partial meniscectomy is often the treatment of choice.

Disclosure: One or more of the authors received payments or services, either directly or indirectly (i.e., via his or her institution), from a third party in support of an aspect of this work. In addition, one or more of the authors, or his or her institution, has had a financial relationship, in the thirty-six months prior to submission of this work, with an entity in the biomedical arena that could be perceived to influence or have the potential to influence what is written in this work. No author has had any other relationships, or has engaged in any other activities, that could be perceived to influence or have the potential to influence what is written in this work. The complete **Disclosures of Potential Conflicts of Interest** submitted by authors are always provided with the online version of the article.

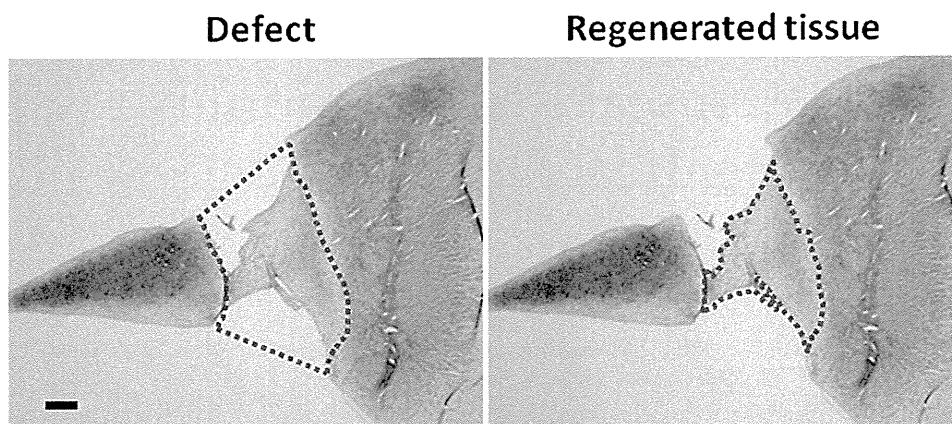


Fig. 1

Method of calculating the quantity of tissue regeneration. The area of the entire defect (D; blue dotted line; left) and the regenerated tissue (R; blue dotted line; right) were calculated. The regenerated tissue-to-defect ratio (R/D) was used to quantify the amount of regenerated meniscal tissue. The ideal quantity of regeneration would result in a value of 1, and incomplete regeneration would result in a value of <1. Scale bar represents 200 μm .

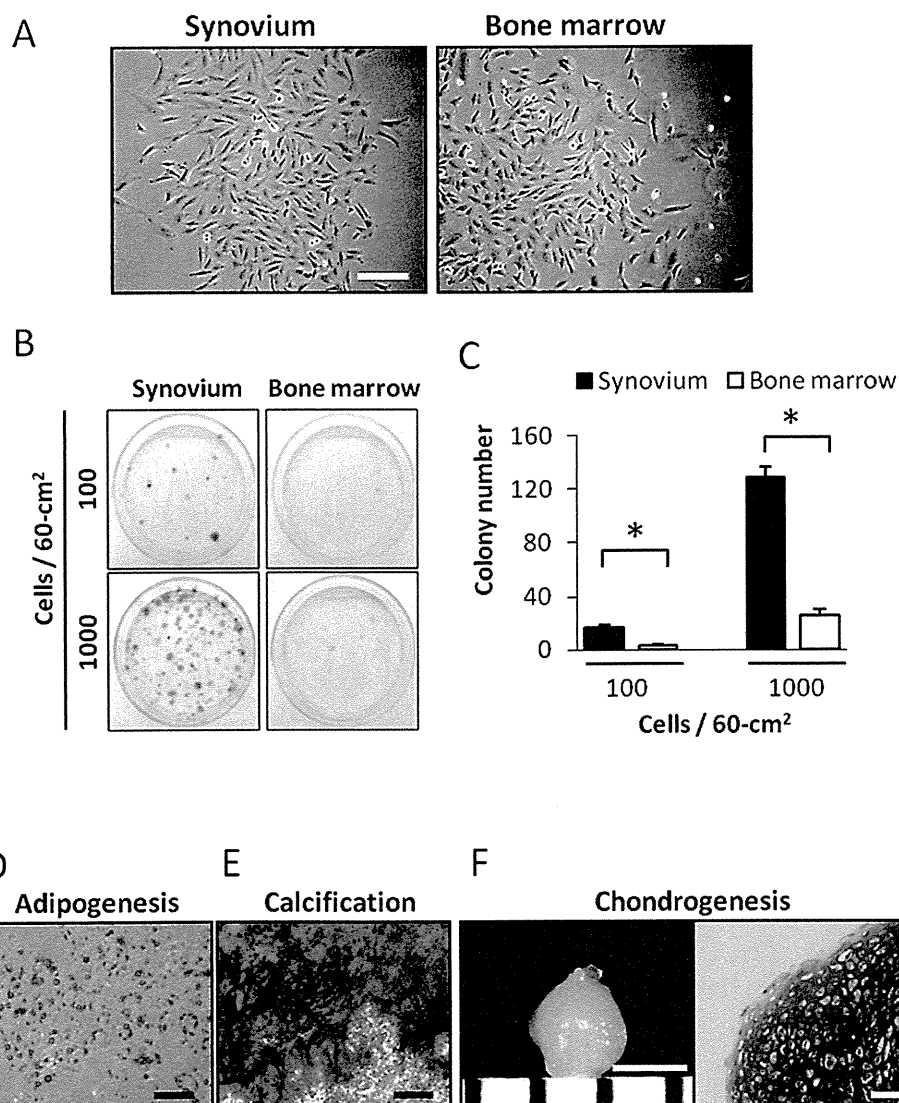


Fig. 2

Figs. 2-A through 2-F Synovial mesenchymal stem cells have high proliferation capacity and multipotentiality. *Synovium* refers to synovial mesenchymal stem cells, and *bone marrow* refers to bone-marrow mesenchymal stem cells. **Fig. 2-A** Histological appearance of synovial mesenchymal stem cells (left) and bone-marrow mesenchymal stem cells (right) at passage 3. Both groups formed monolayers of spindle-shaped cells that adhered to plastic culture dishes. Scale bar indicates 200 μm . **Fig. 2-B** Colony formation of synovial mesenchymal stem cells and bone-marrow mesenchymal stem cells at passage 3. Nucleated cells from synovium and bone marrow were plated at 100 and 1000 cells per 60-cm² dish and cultured for fourteen days (n = 5 cultures each). Culture dishes stained with crystal violet are shown. **Fig. 2-C** Graph showing the number of colonies (>2 mm) per dish at 100 or 1000 cells per 60 cm². *P < 0.01. **Fig. 2-D** Adipogenesis. Adipocyte colonies were stained with oil red O. Scale bar represents 200 μm . **Fig. 2-E** Calcification. Calcified colonies were stained with alizarin red. Scale bar represents 500 μm . **Fig. 2-F** Chondrogenesis. Gross photograph of a pellet (left). Scale bar represents 1 mm. Histological section of the pellet stained with safranin O (right). Scale bar represents 100 μm .



Fig. 3

Figs. 3-A and 3-B Meniscal biopsy and implantation of synovial mesenchymal stem cells. **Fig. 3-A** Intraoperative photograph made following meniscal biopsy. A 1.5-mm-diameter full-thickness cylindrical defect (arrow) was produced in the inner two-thirds of the anterior horn of the medial meniscus. **Fig. 3-B** Intraoperative photograph demonstrating implantation of the synovial mesenchymal stem cells. Two million synovial mesenchymal stem cells in 50 μ L of phosphate-buffered saline solution were placed directly into the meniscal defect of experimental knees with use of a 27-gauge needle. In control knees, the same volume of plain phosphate-buffered saline solution was used.

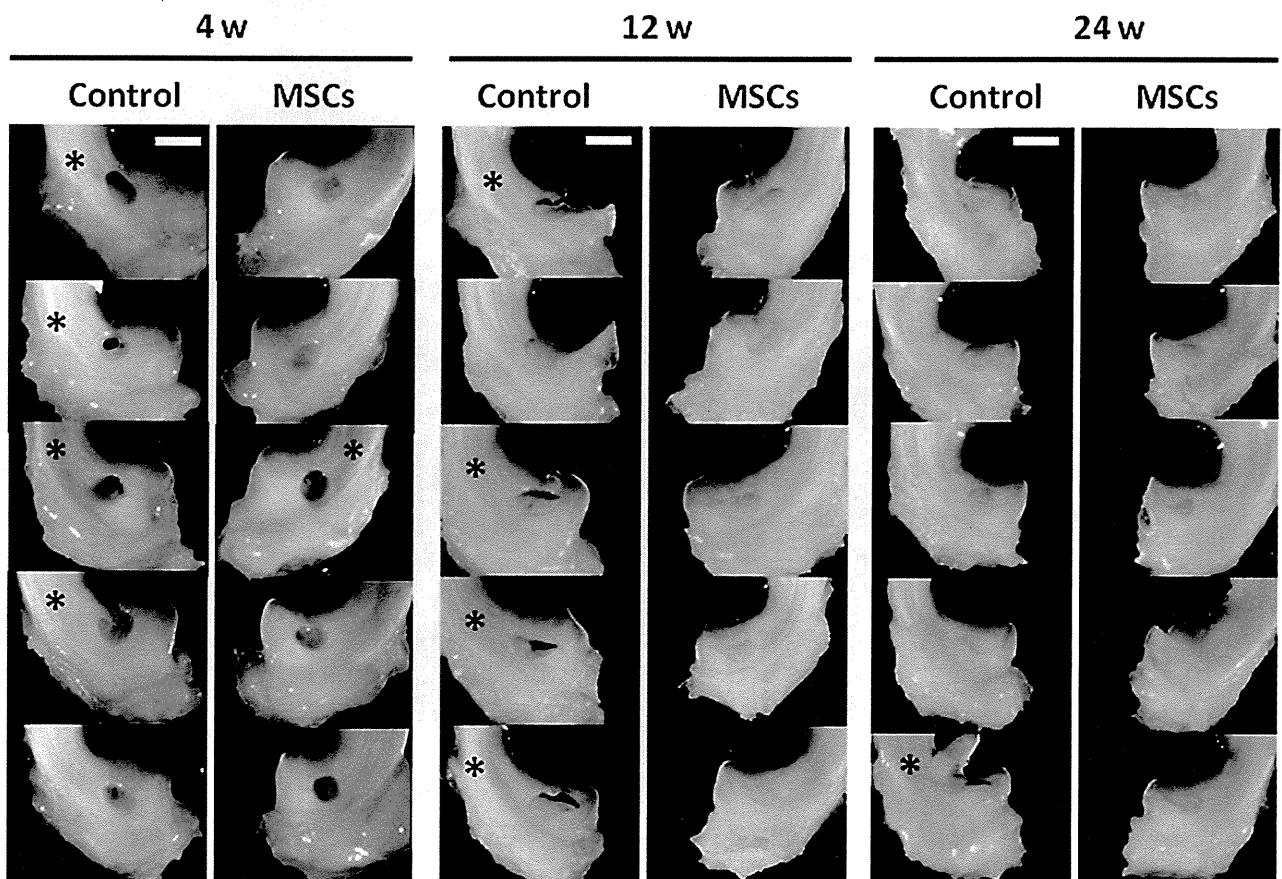


Fig. 4

Synovial mesenchymal stem cells (MSCs) promote meniscal regeneration (macroscopic observation). Macroscopic findings of the meniscus at four, twelve, and twenty-four weeks after the implantation of synovial mesenchymal stem cells. The specimens in which full-thickness grossly visible defects remained are denoted by an asterisk. Scale bar represents 2 mm.

Unfortunately, removal of this important shock absorber leads to accelerated osteoarthritis⁹⁻¹². Thus, new techniques designed to restore meniscal structure and function following injury are needed.

Mesenchymal stem cells are multipotent cells present in mature individuals and readily accessible from peripheral connective tissue sites such as bone marrow^{13,14}, periosteum¹⁵, adipose¹⁶, and the synovial lining of major joints¹⁷. These cells, which are capable of differentiating into osteoblasts, chondrocytes, adipocytes, and myocytes, represent an attractive potential means of regenerating damaged connective tissues including intra-articular structures of the knee, such as the meniscus¹⁸⁻²⁰.

Recent literature has suggested that synovial tissue-derived mesenchymal stem cells may have the potential to aid in healing and regeneration of cartilage injuries, such as those involving the meniscus^{18,20-24}. Synovial mesenchymal stem cells represent an attractive cell source because they can be harvested in a minimally invasive manner from synovial tissue and are easily expanded in

culture^{18,20-22}. In addition, multiple investigators have found that synovial mesenchymal stem cells possess a particularly high capacity for chondrogenic differentiation and proliferation compared with mesenchymal stem cells obtained from other tissues, such as bone marrow or periosteum^{18,20,22}.

Synovial mesenchymal stem cells are also capable of adhering to damaged intra-articular structures such as the meniscus and participating in the repair process in rat models²³⁻²⁶. In rats, however, the animals' innate regenerative capacity limits the ability of the investigator to compare the effect of the cells on tissue regeneration in experimental versus control groups²⁴. In contrast to smaller rodents, the limited inherent regenerative capacity of the rabbit meniscus makes the rabbit a more favorable animal model in which to evaluate meniscal regeneration techniques. Moon et al. found that, following medial meniscectomy, the rabbit meniscus only partially regenerated with primarily fibrous tissue²⁷. More recently, rabbit models have been used to study the effects

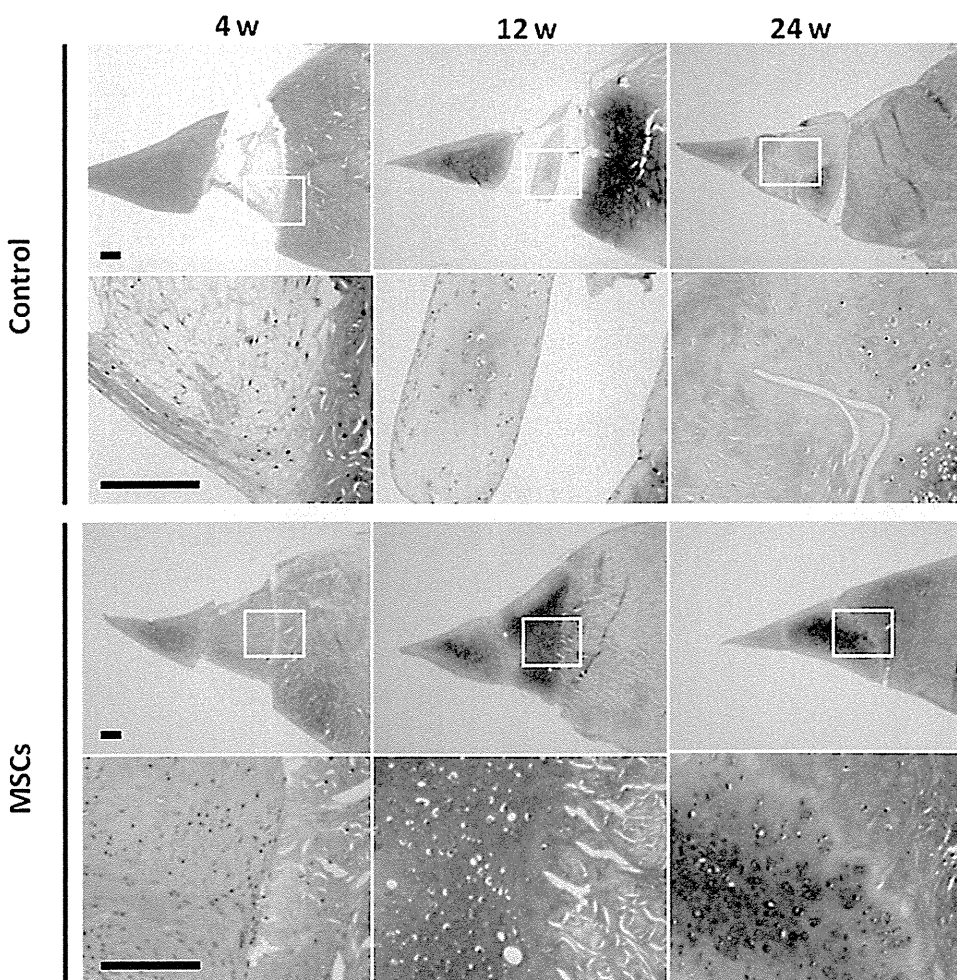


Fig. 5-A

Figs. 5-A through 5-D Synovial mesenchymal stem cells (MSCs) promote the meniscal regeneration (histological observation). **Fig. 5-A** Low and high-power images of representative sections of regenerated meniscus stained with safranin O at four, twelve, and twenty-four weeks after implantation of synovial mesenchymal stem cells. The inset shows the area seen at higher magnification in the photomicrograph below. Scale bars represent 200 μ m. **Fig. 5-B** Low and high-power representative images of the normal meniscus stained with safranin O. Scale bars represent 200 μ m.

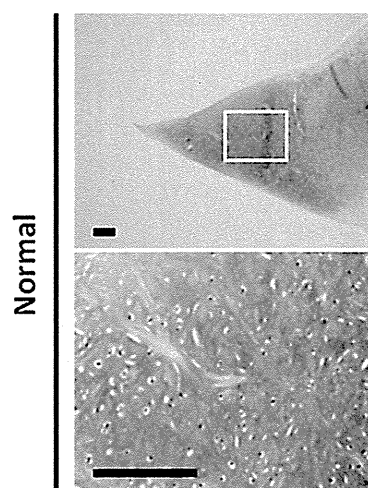


Fig. 5-B

of a variety of surgical interventions aimed at regenerating more normal meniscal tissue with use of scaffolds composed of collagen, polyglycolic acid, or gelatin with or without a potential biological regenerative stimulus²⁸⁻³⁰.

The purpose of this study was to evaluate the effect of synovial mesenchymal stem cell supplementation on meniscal regeneration in a rabbit model of partial meniscectomy.

Materials and Methods

Animals

The experimental protocols were approved by the Scott & White Institutional Animal Care and Use Committee and Texas A&M University Institutional Biosafety Committee. Two mature New Zealand White rabbits were used as cell donors for two experimental groups as follows: a single mature wild-type rabbit served as the synovial donor for Group A (fifteen rabbits), and a single transgenic rabbit bred to ubiquitously express green fluorescent protein (GFP; Kitayama Labes, Nagano, Japan)^{31,32} served as the synovial donor for Group B (four rabbits).

Tissue Harvesting and Mesenchymal Stem Cell Preparation

Through a medial parapatellar surgical approach, the right knee of one mature wild-type New Zealand White rabbit was accessed and synovium from the medial, lateral, and suprapatellar regions of the joint was resected. Bone marrow was harvested from the femoral intramedullary canal for comparison of the proliferation capacity of synovial and bone-marrow mesenchymal stem cells.

Isolated cells were cultured for three passages, and a fluorescent lipophilic tracer, CM-Dil (chloromethylbenzamido Dil; Invitrogen, Carlsbad,

California), was added to the cultured synovial tissue-derived cells (see Appendix). These CM-Dil-labeled cells were then used for implantation in experimental knees of Group-A rabbits to evaluate the effect of synovial mesenchymal stem cell supplementation on the quality and quantity of meniscal regeneration, as detailed below in the section on meniscectomy and cell implantation.

A separate subset of the experiment was performed with use of GFP-positive synovial tissue-derived cells obtained from the knee synovium of a transgenic New Zealand White rabbit bred to ubiquitously express GFP (Kitayama Labes)^{31,32}. These cells were processed as described above without the addition of CM-Dil. These GFP-positive synovial tissue-derived cells were implanted in the experimental knees of Group-B rabbits to track not only implanted cells but also their progeny, as detailed below in the section on meniscectomy and cell implantation.

Colony-Forming Assay

To compare proliferation potentials, synovial tissue-derived cells and bone marrow-derived cells from passage 3 were plated in 60-cm² dishes at densities of 100 or 1000 cells per dish, cultured in complete medium for fourteen days, and stained with 0.5% crystal violet in methanol for five minutes. The number of colonies was then counted. Colonies that were <2 mm in diameter and colonies that were faintly stained were ignored.

In Vitro Differentiation Assay

Isolated synovial tissue-derived cells were cultured under conditions conducive to adipogenesis, calcification, and chondrogenesis to assess for multipotentiality (see Appendix).

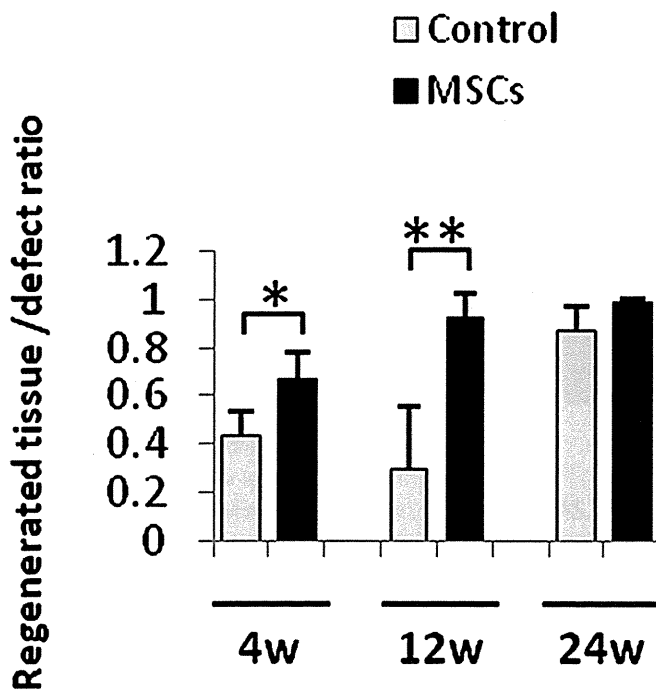


Fig. 5-C

Fig. 5-C Regenerated tissue-to-defect ratios are displayed as the mean and the standard deviation for synovial mesenchymal stem cell (MSCs) and control groups at each end point. *The difference between the groups was significant ($p < 0.05$). **The difference between the groups was significant ($p < 0.01$).

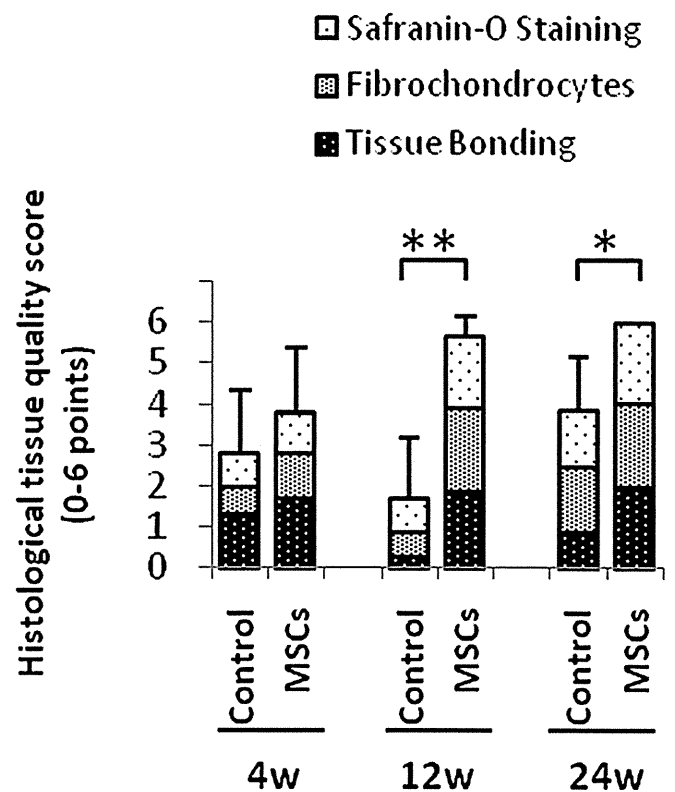


Fig. 5-D

Fig. 5-D Results of the histological scoring system for regenerated meniscus. The scores are displayed as the mean and the standard deviation. *The difference between the groups was significant ($p < 0.05$). **The difference between the groups was significant ($p < 0.01$).

Meniscectomy and Implantation of Synovial Mesenchymal Stem Cells

Nineteen additional mature New Zealand White rabbits were divided into two groups, consisting of fifteen rabbits in Group A and four in Group B.

Group A

With the animal under general anesthesia, each knee was approached through a medial parapatellar arthrotomy, maximally flexed, and a reproducible 1.5-mm-diameter full-thickness cylindrical defect was produced in the avascular inner two-thirds³³ of the anterior portion of the medial meniscus with use of a biopsy punch (Miltex, York, Pennsylvania).

With the tibial joint surface facing upward, 2×10^6 CM-Dil-labeled synovial tissue-derived mesenchymal stem cells in 50 μ L of phosphate-buffered saline solution (PBS)³⁴ were placed directly into the meniscal defect in each of the right knees with use of a 27-gauge needle. Knees were then held stationary for ten minutes during wound closure. In left knees, the same volume of plain PBS was implanted as a control, and the knees were once again held stationary for ten minutes.

Capsule and skin were closed in layers with absorbable suture. Rabbits were allowed to move freely in their cages. Medial menisci from both knees were harvested at four, twelve, and twenty-four-week end points.

Group B

A similar procedure was performed on the remaining four rabbits, with the goal of tracking the fate of implanted mesenchymal stem cells and their progeny. For this purpose GFP-positive synovial mesenchymal stem cells were implanted in

the right knees in the same manner as those in Group A. The same volume of PBS was placed in the left knees once again. Medial menisci from the right and left knees were then harvested at one-day, one-week, four-week, and twelve-week end points.

Histological Analysis

Meniscal specimens from Group A were fixed in 4% paraformaldehyde, decalcified, and embedded in paraffin. Specimens were then sectioned into slices 5 μ m thick in the radial plane. The quantity and quality of regenerated meniscal tissue were then evaluated as follows:

Tissue Quantity Analysis

The quantity of tissue regeneration was evaluated with use of random tissue sections obtained from the central portion of the meniscal defect as shown in Figure 1 and described in detail in the Appendix. The area of the original defect (D) and the area occupied by regenerated tissue inside the defect (R) were calculated with use of Photoshop CS3 software (Adobe Systems, San Jose, California). Tissue regeneration is expressed as the ratio of regenerated tissue area to the entire defect area (regeneration ratio = R/D).

Tissue Quality Scoring Analysis

A quantitative scoring system evaluating three dimensions of meniscal regeneration was used (see Appendix)³⁰. Sections to be scored were stained with safranin O. Histological scoring was performed by two investigators blinded to treatment category.

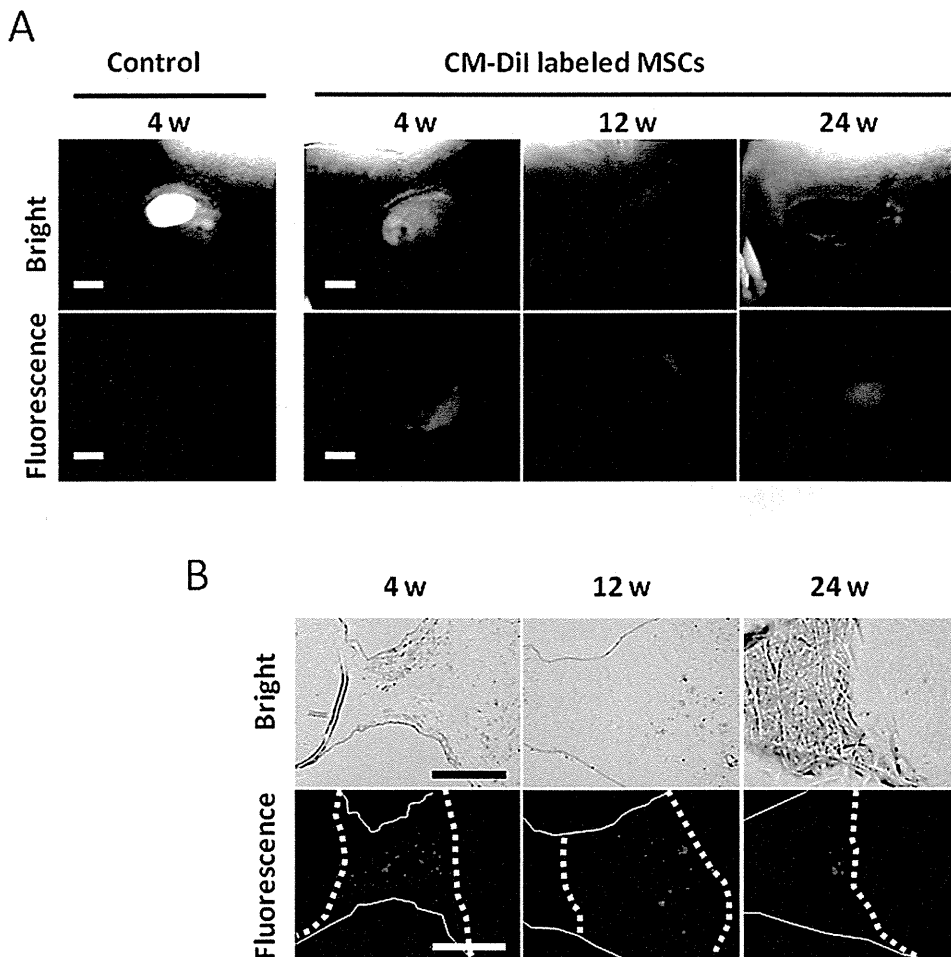


Fig. 6

Figs. 6-A and 6-B CM-Dil-labeled synovial mesenchymal stem cells (MSCs) adhere to sites of meniscal injury and remain at twenty-four weeks. Representative macroscopic appearance (**Fig. 6-A**) and histological sections (**Fig. 6-B**) of the meniscal defect after implantation of CM-Dil-labeled synovial mesenchymal stem cells under bright light (top) and fluorescence (bottom). In the histological sections (**Fig. 6-B**), the white solid line indicates the outer edge of the meniscus, and the white dotted line indicates the border between native meniscus and regenerated tissue. Scale bar represents 400 μ m.

Fluorescent Microscopy

Photographs of the gross and microscopic appearance of each Group-A meniscal specimen were made under fluorescence to demonstrate the presence or absence, as well as relative density, of CM-Dil-labeled synovial mesenchymal stem cells within the defects and surrounding intact meniscal tissue.

To determine the fate of the implanted GFP-positive synovial mesenchymal stem cells and their progeny in Group-B rabbits, menisci from both knees were harvested, fixed in 4% paraformaldehyde, and transferred to 20% sucrose solution. Specimens were flash-frozen, cut in a cryostat, and observed under fluorescent microscopy.

Immunohistochemistry for Type-I and Type-II Collagen

Frozen sections from the menisci of Group-B rabbits were also used to detect type-I and type-II collagen synthesis with use of standard immunohisto-

chemistry techniques (see Appendix). Background nuclei were counterstained with 4', 6-diamidino-2-phenylindole dihydrochloride (DAPI).

Statistical Methods

An a priori power calculation was performed with use of mean and standard deviation assumptions based on previously published data³⁰. A sample size of five rabbits was found to be sufficient to detect a difference of 3 points in the tissue quality score at the twelve-week end point, with a power of 89% at a significance level of 0.05. The Mann-Whitney U test was used to compare synovial mesenchymal stem cells and control groups at each period. P values of <0.05 were considered significant.

Source of Funding

Funding for this study was provided by an internal institutional grant from the Scott & White Research Grants Program as well as a grant from the National Institutes of Health (NIH/NCRR grant P40 RR 17447).

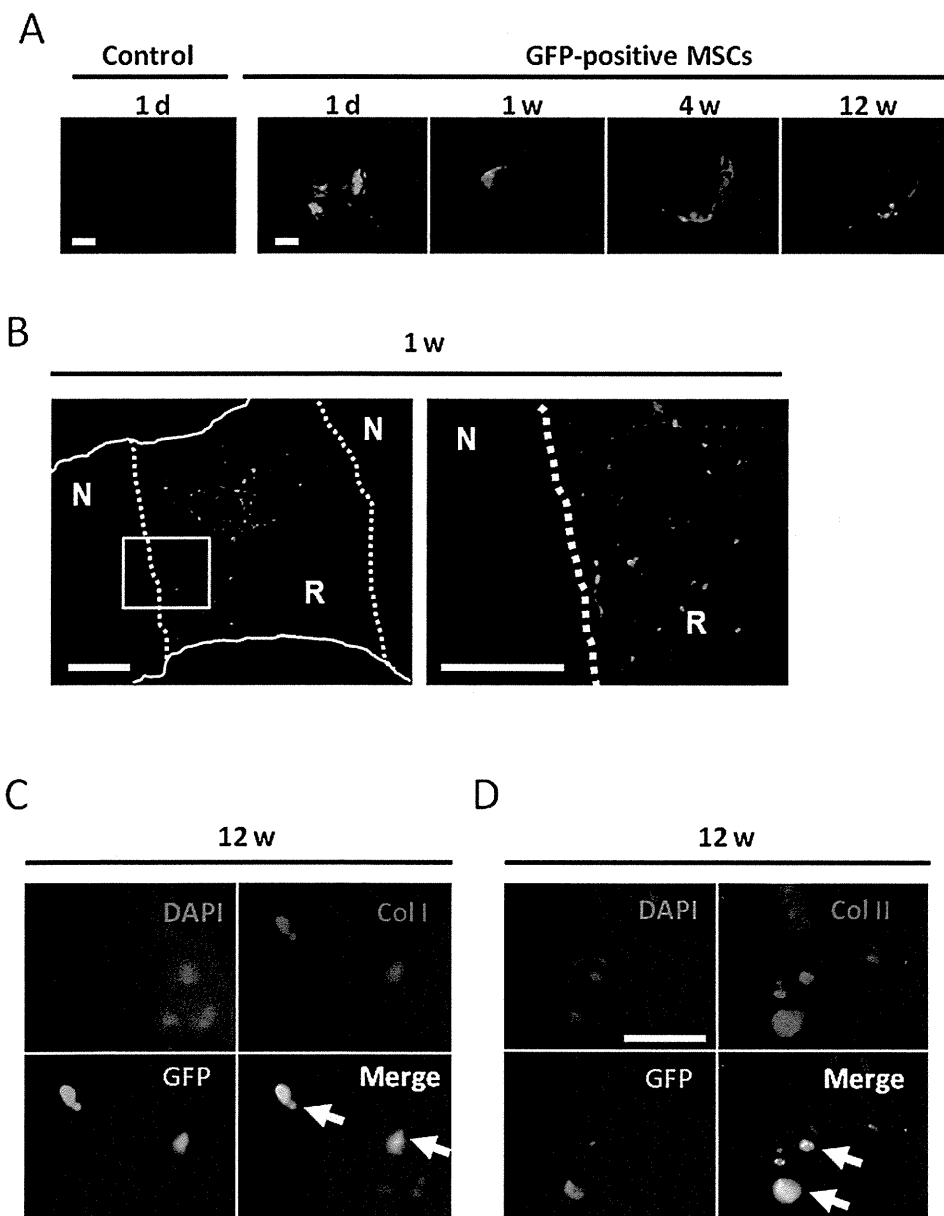


Fig. 7

Figs. 7-A and 7-B Green fluorescent protein (GFP)-positive synovial mesenchymal stem cells (MSCs) adhere to sites of meniscal injury in experimental knees, where they produce type-I and type-II collagen. Representative macroscopic appearance (**Fig. 7-A**) and histological sections (**Fig. 7-B**) of the meniscal defect one day to twelve weeks after the implantation of GFP-positive synovial mesenchymal stem cells under fluorescence. In the histological sections (**Fig. 7-B**), the white solid line indicates the outer edge of the meniscus. The white dotted line indicates the border between native meniscus (N) and regenerated tissue (R). The inset shows the area seen at higher magnification in the photomicrograph on the right. The scale bars represent 200 μm . **Figs. 7-C and 7-D** Fluorescent images of the regenerated meniscus at twelve weeks after implantation of GFP-positive synovial mesenchymal stem cells. The sections were immunostained with anti-type-I collagen (**Fig. 7-C**) and anti-type-II collagen (**Fig. 7-D**). Nuclei were counterstained with DAPI (4', 6-diamidino-2-phenylindole dihydrochloride; blue) to demonstrate the cellular background (GFP-positive cells as well as cells not expressing GFP). GFP-positive cells are shown in green (bottom left), and type-I collagen-producing cells (**Fig. 7-C**) and type-II collagen-producing cells (**Fig. 7-D**) are shown in red (top right). Arrows in merge (bottom right) indicate double-positive cells of GFP and type-I collagen (**Fig. 7-C**) or type-II collagen (**Fig. 7-D**). Scale bar represents 25 μm . Col I = type-I collagen, and Col II = type-II collagen.

TABLE I Regenerated Tissue-to-Defect Ratio

	Ratio*	P Value
4 weeks		
Control	0.44 ± 0.10	0.028†
MSC	0.67 ± 0.11	
12 weeks		
Control	0.29 ± 0.27	0.009‡
MSC	0.93 ± 0.10	
24 weeks		
Control	0.87 ± 0.10	0.077
MSC	0.98 ± 0.03	

*Regenerated tissue-to-defect ratios (range, 0 to 1) are given as the mean (and standard deviation) for synovial mesenchymal stem cell (MSC) and control groups at each end point. †The difference between the groups was significant ($p < 0.05$). ‡The difference between the groups was significant ($p < 0.01$).

Results

Synovial Mesenchymal Stem Cells Have High Proliferation Capacity and Multipotentiality

Abundant multipotent cells were isolated from the synovial tissue of the initial donor rabbit. Isolates produced spindle-shaped cells that adhered to plastic culture dishes under standard conditions, and appeared morphologically similar to the cultured bone-marrow mesenchymal stem cells (Fig. 2-A). While both synovial and bone-marrow mesenchymal stem cells were capable of forming single-cell colonies, the synovial mesenchymal stem cells demonstrated greater colony-forming potential when plated at densities of 100 cells per 60 cm² and 1000 cells per 60 cm² (Figs. 2-B and 2-C).

Isolated synovial mesenchymal stem cells were capable of differentiation into adipocytes and chondrocytes, and were calcified under the proper conditions (Figs. 2-D, 2-E, and 2-F). In adipogenic medium, colonies stained well with oil red O (Fig. 2-D). In calcification medium, colonies produced abundant calcium (Fig. 2-E). In chondrogenic medium, smooth glistening pellets, which stained diffusely with safranin O, were produced (Fig. 2-F). Thus, the isolated synovial mesenchymal stem cells met the requirements for multipotent mesenchymal stromal cells as set forth by Dominici et al.³⁵

Locally Implanted Synovial Mesenchymal Stem Cells Promote Meniscal Regeneration

A representative photograph of the in vivo 1.5-mm-diameter full-thickness meniscal biopsy of the avascular portion of the anterior horn of the medial meniscus is shown in Figure 3-A. Application of either synovial mesenchymal stem cells suspended in PBS (right knees) or PBS alone (left knees) is demonstrated in Figure 3-B.

A gross representation of regenerated meniscal tissue within the 1.5-mm cylindrical defects is shown in Figure 4. In the control knees, grossly visible, full-thickness defects remained in

four of five specimens at four and twelve weeks (asterisks in Figure 4). In knees supplemented with synovial mesenchymal stem cells, however, such defects remained in only one specimen at four weeks and none at twelve weeks. The macroscopic difference between mesenchymal stem cell and control groups is less dramatic at twenty-four weeks, by which time four of five defects in control knees and five of five defects in knees supplemented with mesenchymal stem cells were completely covered with at least partial-thickness tissue on gross inspection.

Representative sections of regenerated meniscus stained with safranin O at four, twelve, and twenty-four weeks after implantation of synovial mesenchymal stem cells, as well as sections of normal meniscus stained with safranin O, are shown in Figures 5-A and 5-B. The quantity of regenerated meniscal tissue was greater when measured histologically in knees receiving synovial mesenchymal stem cells, reaching significance at four and twelve weeks ($p < 0.05$) (Fig. 5-C, Table I). By twelve weeks, an average of >90% of the cylindrical defect had filled in with regenerated tissue in knees supplemented with synovial mesenchymal stem cells compared with <30% in controls.

The quality of meniscal regeneration was also superior in knees supplemented with synovial mesenchymal stem cells at all end points, achieving significance at twelve and twenty-four weeks (Fig. 5-D, Table II). By twenty-four weeks, all menisci from knees treated with synovial mesenchymal stem cells scored the highest possible score in each of the three quality domains measured—staining with safranin O, existence of fibrochondrocytes, and extent of bonding between regenerated tissue and the borders of the meniscal defect.

Synovial Mesenchymal Stem Cells Adhere to Sites of Meniscal Injury and Differentiate into Type-I and II Collagen-Producing Cells

Gross and histologic fluorescence imaging revealed the presence of CM-DiI-labeled cells in high concentration within the meniscal

TABLE II Histological Tissue Quality Score

	Score*	P Value
4 weeks		
Control	2.8 ± 1.5	0.29
MSC	3.8 ± 1.6	
12 weeks		
Control	1.7 ± 1.5	0.008†
MSC	5.7 ± 0.4	
24 weeks		
Control	3.9 ± 1.3	0.021‡
MSC	6.0 ± 0	

*Results of histological scoring system (range, 0 to 6) for regenerated meniscus. The values are given as the mean and the standard deviation. †The difference between the mesenchymal stem cell (MSC) and control groups was significant ($p < 0.01$). ‡The difference between the groups was significant ($p < 0.05$).